Investigation of the Oxygen Depletion Properties of Novel Oxygen-Scavenging Plastics

Jen-Taut Yeh,[1,3] Li Cui,[2] Chang-Jung Chang,[1] Tao Jiang,[2] Kan-Nan Chen[4]

[1]*Graduate School of Polymer Engineering, National Taiwan University of Science and Technology, Taipei, Taiwan*
[2]*Faculty of Chemistry and Material Science, Hubei University, Wuhan, People's Republic of China*
[3]*Institute of Textile and Material, Wuhan University of Science and Engineering, Wuhan, People's Republic of China*
[4]*Department of Chemistry, Tamkang University, Tamsui, Taiwan*

Received 22 July 2007; accepted 29 December 2007
DOI 10.1002/app.28674
Published online 17 July 2008 in Wiley InterScience (www.interscience.wiley.com).

ABSTRACT: The oxygen depletion and tensile properties of EVA resins blended with varying compositions and sizes of iron (Fe), modified iron (MFe) and ascorbic acid (Vc) oxygen scavengers were systematically investigated. After blending Vc together with varying sizes of MFe in EVA resins, "synergistic" oxygen depletion properties were found in each $E_{VcMFe\text{-}30}$, $E_{VcMFe\text{-}5}$, and $E_{VcMFe\text{-}1}$ series samples, as their weight ratios of Vc to MFe are between 3/7 to 5/5, 3/7 to 7/3 and 1/9 to 9/1, respectively. The oxygen depletion rates of E_{VcMFe} series samples increase significantly as the particle sizes of MFe powders reduce. In fact, the oxygen-scavenging resins with better oxygen depletion properties always result in lower peroxide values for modeled food samples stored in the airtight flasks of E_{VcMFe} series samples. Further tensile experiments show that the tensile properties of the E_{VcMFe} series samples increase significantly as their Vc loadings or the sizes of the MFe powders reduce. To understand these interesting oxygen depletion, lipid oxidation, and tensile properties of E_{VcMFe} series samples, SEM and EDX analysis of the compositions on the surfaces of E_{VcMFe} series samples were performed. Possible mechanisms accounting for these interesting properties of E_{Vc}, E_{Fe}, E_{MFe}, and E_{VcMFe} series samples are proposed. © 2008 Wiley Periodicals, Inc. J Appl Polym Sci 110: 1420–1434, 2008

Key words: plastics; compounding; blends

INTRODUCTION

The potential for spoilage of all foods at some rate may occur at any stages during storage, especially for the lipid oxidation food.[1–4] Fat and oils are well-known lipid oxidation foods that undergo pronounced oxidative changes at elevated temperature during storage. These oxidative changes spoil the quality of fats and oils present in foods and result in safety and health problems. As reported by several investigations,[5–9] storage condition (e.g., oxygen concentration, temperature, and light), degree of unsaturation of the fatty acids, and the presence of anti- and prooxidants or enzymes can significantly affect the oxidation rates of lipid oxidation foods. In which, oxidation of unsaturated fatty acids is the most intensively studied nonenzymatic deteriorative reaction of lipid oxidation food.[5] As suggested by Morrissey and coworkers,[7] during the course of lipid oxidation, fatty acyl radicals ($R^{\bullet}$) can be easily formed after removing the hydrogen from the methylene carbon in the fatty acid (RH), wherein the concentrations of $R^{\bullet}$ are expected to increase with the concentrations of double bonds present in the fatty acid. The fatty acyl radicals ($R^{\bullet}$) then react rapidly with O_2 to form the peroxyl radicals ($ROO^{\bullet}$), which will preferentially oxidize other unsaturated fatty acids. The means to inhibit and/or reduce the lipid oxidation rates of fats and oils present in foods include introduction of exogenous antioxidants,[10–11] controlling the storage conditions, and the avoidance of oxidative processing stages.

"Passive" and "active" packaging technologies have been used to reduce the oxygen contents and to improve the shelf life of food contained in package for more than 20 years.[12] Barrier plastic materials, such as poly(ethylene terephthalate), polyamide, polyvinylidiene chloride, and ethylene-vinyl alcohol copolymer are often used as key components in the "passive" packaging technology[13–25] to enhance the oxygen permeation resistance of plastic packages. Nevertheless, barrier plastic packaging materials cannot prevent permeation of oxygen completely. By using the active packaging, quality changes of oxygen-sensitive foods can often be minimized,[26–29] wherein the oxygen scavenger is often introduced into the active packaging. In contrast to the barrier plastic materials, oxygen scavengers can react with oxygen that was trapped in the plastic packaging materials or permeated into the packages,[26] and

Correspondence to: J.-T. Yeh (jyeh@tx.ntust.edu.tw).

hence, offer safety and savings.[27] Various organic and inorganic types of oxygen scavengers have being used in the active packaging technology. Iron, sodium hydrosulfite, platinum materials are well-known inorganic oxygen scavengers.[30–33] In contrast, yeast, ascorbic acid (i.e., vitamin C), enzyme, and photosensitive dye were often used as organic oxygen scavengers in the literatures.[34–37] In which, iron powder and ascorbic acid are the most often used oxygen scavengers in the food packaging. Iron powders are normally used with dry foods in the form of "sachet," and have a potential risk of being accidentally ingested.[39–40] The "Ageless" iron-based sachets were introduced by Mitsubishi Chemical Corporation (Tokyo, Japan) in the late 1970s,[38] which have been and continue to be the in-package oxygen-scavenging technology of commercial choice since then. However, iron-based oxygen scavenger reacts with oxygen and loses its ability of oxygen depletion quickly, when the oxidation reaction is performed in an environment of sufficient water vapor and oxygen.[39] In contrast to iron powders, the ascorbic acid oxygen scavengers are often added directly into liquid food or beverage as an efficient oxygen scavenger, however, its oxygen depletion rate is slow unless it is catalyzed by the transition metals. As reported by several investigators,[40–42] the oxygen removing rates of the ascorbic acid can be accelerated by the presence of transition metal ions such as Cu^{2+}, Fe^{2+}, etc. However, after oxidization, the ascorbic acid present in solutions turns into light-brown color and, hence, affects the appearance of the products.

Numerous patents[20–30] and some conference proceedings[43] give sufficient detail to allow a comparison of the systems reported. For example, W. R. Grace and Co. has applied patents for the use of ascorbic acid (Vc) dispersed into plastics, such as the common heat-seal plastics of closure liners. In fact, oxygen-scavenging packaging has been applied in packs recently. Some commodities are appeared in the world.[44–45] Some of these oxygen-scavenging packaging contains iron in their structure, whereas others are based on organic compounds that absorb oxygen after being activated, normally by ultra-violet light.[46–48] However, as far as we know, very few investigations of the chemistry and composition of oxygen-scavenging plastic films have been published in peer-reviewed journals. Our recent investigation[48] found that the oxygen depletion rates of modified iron powders filled EVA series samples (E_{MFe}) are much faster than those of E_{Vc} and E_{Fe} series samples filled with the same weight loadings of ascorbic acid and pure iron powders, respectively, wherein the E_{Vc} series samples exhibit slightly slower oxygen depletion rates than those of the corresponding E_{Fe} series samples. After blending Vc together with modified iron (MFe) powder oxygen scavenger compounds in EVA resins, a "synergistic" effect on the oxygen depletion properties of the E_{VcMFe} samples was observed when the weight ratios of Vc to MFe oxygen scavengers are between 3/7 to 5/5. Further SEM and EDX analysis of the compositions on the surfaces of E_{VcMFe} series samples indicate that the ascorbic acid powders were found surrounding but not over-wrapping on the surfaces of the MFe powders as the weight ratios of Vc to MFe present in the E_{VcMFe} specimens are between 3/7 and 5/5. However, it is not completely clear what accounts for these interesting oxygen depletion properties of the E_{Vc}, E_{Fe}, E_{MFe}, and E_{VcMFe} plastics active materials.

In this article, iron powder with varying sizes and ascorbic acid were chosen as the main components of oxygen scavenger compounds to blend with EVA resins to prepare the oxygen-scavenging plastics, wherein the EVA plastic carrier is a high oxygen- and water-permeable material. The main objective of this study is to investigate the influences of compositions and sizes of the modified iron powders on the oxygen depletion and lipid oxidation properties of the Vc/MFe oxygen scavenger compounds filled E_{VcMFe} oxygen-scavenging plastics. It is interesting to note that the E_{VcMFe} samples prepared in this study can be used as efficient oxygen-scavenging resins to prevent modeled food samples from lipid oxidation. Possible mechanisms accounting for these interesting oxygen depletion, lipid oxidation, and tensile properties of noble oxygen scavenger filled E_{VcMFe} oxygen-scavenging plastics are proposed.

EXPERIMENTAL

Materials and sample preparation

The ethylene vinyl acetate (EVA) resin with a trade name of UE638 was quoted with a 28 wt % of VA content and 18 g/10 min melt indexes by Union Carbide Corporation, Taiwan branch. The ascorbic acid and iron powders of different particle sizes used as the oxygen scavengers were purchased from Tianjin Chemical and Chengdu Sagewell Science Corporation, respectively. To accelerate the oxygen removing properties of the iron powders of varying sizes, the powders were mixed with 20% sodium chloride (NaCl) solution at a weight ratio of 40 : 1. Before blending with EVA resins, NaCl-treated iron powders of varying sizes were then dried in a vacuum oven at 80°C for 4 h to remove the residual water. The NaCl-treated iron powders of varying sizes will be referred to as the modified iron (MFe) powders in the following discussion. The oxygen-absorbable resins were then prepared by melt-blending EVA resins with varying amounts of MFe and ascorbic acid powders, respectively. For comparison

TABLE I
The Compositions of E_{VcMFe} Series Specimens with Varying Particle Sizes of Modified Iron Powders

Sample		EVA (phr)	V_C (phr)	MFe (phr)		
				30 μm	5 μm	1 μm
$E_{VcMFe-30}$	$E_{MFe10-30}$	100		10		
	$E_{Vc1MFe9-30}$	100	1	9		
	$E_{Vc3MFe7-30}$	100	3	7		
	$E_{Vc5MFe5-30}$	100	5	5		
	$E_{Vc7MFe3-30}$	100	7	3		
	$E_{Vc9MFe1-30}$	100	9	1		
$E_{VcMFe-5}$	$E_{MFe10-5}$	100			10	
	$E_{Vc1MFe9-5}$	100	1		9	
	$E_{Vc3MFe7-5}$	100	3		7	
	$E_{Vc5MFe5-5}$	100	5		5	
	$E_{Vc7MFe3-5}$	100	7		3	
	$E_{Vc9MFe1-5}$	100	9		1	
$E_{VcMFe-1}$	$E_{MFe10-1}$	100				10
	$E_{Vc1MFe9-1}$	100	1			9
	$E_{Vc3MFe7-1}$	100	3			7
	$E_{Vc5MFe5-1}$	100	5			5
	$E_{Vc7MFe3-1}$	100	7			3
	$E_{Vc9MFe1-1}$	100	9			1

purposes, MFe powders of varying sizes together with the ascorbic acid powders were melt-blended with EVA resin to improve the oxygen depletion properties of oxygen-scavenger-added EVA resins, since MFe powders are known as the efficient catalysts for ascorbic acid to remove oxygen. Before melt-blending, ascorbic acid and EVA was dried under vacuum at 40°C for 24 h, and then blended with varying compositions of oxygen scavengers using a SU-70 Plasti-Corder Mixer, which was purchased from Suyuan Science and Technology Corporation (Chang Zhou, China). The 70-mL Plasti-Corder Mixer is equipped with a corotating, intermeshing twin screw with a diameter of 30 mm and L/D ratio of 10. During each compounding process, the Plasti-Corder Mixer was operated at 90°C and a screw speed of 100 rpm for 10 min. To prevent EVA from thermal and oxygen degradation, mixing of EVA and the oxygen scavenger compounds was performed in flow nitrogen environment at 90°C. The compositions of oxygen-absorbable EVA resins prepared in this study are summarized in Table I. The prepared EVA resins were then hot-pressed at 90°C and 10 MPa for 10 min and then cooled at room temperature. The film thickness of the EVA hot-pressed films is about 0.3 mm.

Oxygen depletion experiments

The film specimens used in each oxygen depletion experiments were prepared by sectioning the hot-pressed films prepared above into a rectangular slices with a dimension of 3 cm × 5 cm × 0.03 cm. A 300-mL conical flask filled with 200 mL of water was used for the oxygen depletion experiments. The slice specimens were hung on a thread, which was clamped on a conical flask by a sealing stopple. Under such circumstance, the relative humidity present in the airtight flask was controlled at 100% relative humidity. The residual oxygen concentrations present in the conical flask were examined using a China 9800T Gas Chromatography instrument equipped with a thermal conductivity detector, which was purchased from Shanghai Kechuang Chromatograph Instruments (Shanghai, China). The column used for the separation of nitrogen and oxygen contained in the conical flask has an inside diameter of 0.5 mm and a length of 2 m, wherein the column was packed with molecular sieves of 5 Å (60–80 mesh). Helium flowing at 15 mL/min was used as the carrier gas. The injection, column, and detector temperature was set at 70, 100, and 90°C, respectively. All the oxygen depletion tests were carried out at 30°C and 100% relative humidity for varying amounts of time.

Mechanical properties analysis

The tensile properties of the hot-pressed EVA specimens were determined using a Shimadzu tensile testing machine model AG-10KNA at 28°C and a crosshead speed of 200 mm/min. A 35-mm gauge length was used during each tensile experiment. The dimensions of the dog-bone shaped specimens were prepared according to ASTM D 638 type IV standard. The values of tensile strength and elongation at break were obtained based on the average tensile results of at least five tensile specimens.

Thermal properties

The thermal properties of EVA and $E_{VcMFe-1}$ series specimens were determined at 25°C using a TA Q100 differential scanning calorimetry (DSC). All scans were carried out at a heating rate of 10°C/min and under flowing nitrogen at a flow rate of 50 mL/min. The instrument was calibrated using pure indium. Samples weighing about 15 mg were placed in standard aluminum sample pans for percentage crystallinity (W_c) measurements. The W_c values of EVA resins were estimated with baselines drawn from 30 to 90°C and with a perfect heat of fusion of polyethylene of 293 J/g.[49] The ΔH_f values of the EVA and $E_{VcMFe-1}$ series specimens are about the same within experimental error, which yield roughly 3–4% of W_c values. Apparently, the W_c values of the EVA and $E_{VcMFe-x}$ series specimens prepared in this study are very small and roughly the same within experimental error.

Particle size and morphology analysis

To understand the distribution of oxygen scavenger powders in the matrices of EVA film specimens, the oxygen-absorbable EVA specimens were observed using a HITACHI S-3000N scanning electron microscope (SEM). The specimens were gold-coated at 15 keV for 30 s before SEM examinations. The compositions on the surface of the film specimens were determined with a HORIBA 7201-H energy dispersive X-rays (EDX) equipped on the SEM described earlier.

Analysis of the lipid oxidation of a modeled food sample

The modeled food samples used for lipid oxidation experiments were prepared first by mixing water, flour, and seed oil thoroughly at the weight ratio of 3 : 1 : 3. The thoroughly mixed mixtures were heated in an oven at 80°C for 30 min to remove the residual water and then used as the modeled food samples for lipid oxidation experiments. Before lipid oxidation experiments, 5-g modeled food samples were hung in airtight conical flasks with EVA and $E_{VcMFe-x}$ series film specimens at 30°C and 100% relative humidity for varying amounts of time, wherein the dimension of EVA and $E_{VcMFe-x}$ series film specimens is 3 cm × 5 cm × 0.03 cm. The lipid oxidation degrees of modeled food samples were determined using sodium thiosulfate-iodine ($Na_2S_2O_3$-I_2) titration method to estimate the peroxide value (POV) as suggested by GB5008-56 standard. Before $Na_2S_2O_3$-I_2 titration, the modeled food samples prepared above were ground and placed in petroleum ether solvent for 6 h to extract the lipid using a Soxhlet extractor at 25°C. The extracted lipids were then dried at 95°C in a vacuum oven for 2 h to remove the residual solvent. Five grams of extracted lipid was then dissolved in 30 mL acetic acid-chloroform solution (3 : 2, v/v) in the conical flask with a lid. During the course of dissolution, the lipid solutions were well mixed at 25°C for 5 min using a magnetic stir, and then mixed with 0.5 mL of saturated aqueous potassium iodide (KI) for another 10 min. KI was then oxidized by the extracted lipids and turned to brown I_2. Before titration with 0.01 mol/L sodium thiosulfate ($Na_2S_2O_3$), the dark-brown lipid solution was added with 30 mL of distilled water to dilute its color for easiness of further titration. Half milliliter of starch indicator was added until the color of the lipid solution turned from brown to straw yellow. The titration continued until the blue color of the starch-added lipid solution disappeared, at which all the liberated I_2 was reduced by $Na_2S_2O_3$.[50]

All lipid oxidation experiments were performed under protection from light. The blank test was experienced using the model food stored for 0 h. The POV (mequiv/kg) of the food sample was then calculated according to the following equation.

$$\text{Peroxide value (POV)} = \frac{(V - B) \times N \times 1000}{W} \quad (1)$$

wherein V and B are the volume (mL) of the 0.01N sodium thiosulfate solution used in the lipid oxidation and blank tests, respectively; N is the mole concentration of sodium thiosulfate solution and W is the weight (g) of extracted lipid.

RESULTS AND DISCUSSION

Morphology and composition analysis of the oxygen-scavengers-filled EVA specimens

Typical SEM micrographs and EDX analysis of the compositions on the surfaces of pure EVA, E_{vc}, E_{Fe}, and E_{MFe} series samples are summarized in Figure 1. The iron (Fe), modified iron (MFe), and ascorbic acid (Vc) powders were not significantly aggregated in the E_{vc}, E_{Fe10}, and E_{MFe10} samples, respectively. However, in comparison with the Vc powders, Fe and MFe powders are present as darker particles in the EVA matrix, wherein the average particle sizes of Vc powders are about 1–5 μm that are relatively smaller than those of the Fe (MFe) powders with original particle sizes of about 30, 5, and 1 μm, respectively (see Fig. 1). In contrast, a thin, slightly transparent layer of NaCl was found covering the MFe but not the Fe powders. As expected, the EDX composition analysis of the MFe particles present on the surfaces of the E_{MFe10} specimens indicates that

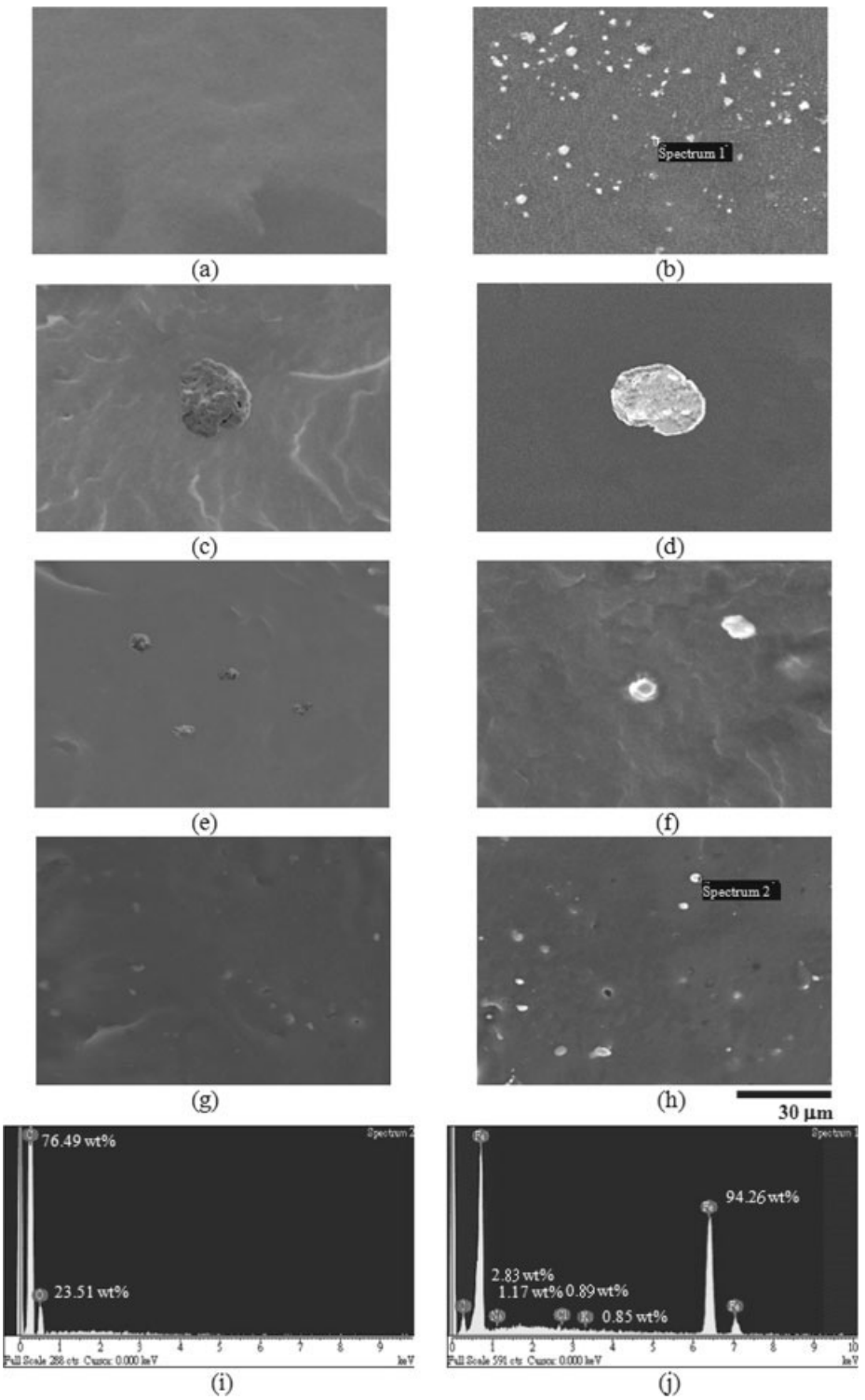

Figure 1 SEM micrographs of the fracture surfaces of (a) EVA, (b) E_{vc10}, (c) $E_{Fe10\text{-}30}$, (d) $E_{MFe10\text{-}30}$, (e) $E_{Fe10\text{-}5}$, (f) $E_{MFe10\text{-}5}$, (g) $E_{Fe10\text{-}1}$, (h) $E_{MFe10\text{-}1}$ specimens and EDX composition analysis of the particles present in (i) E_{vc10} and (j) $E_{MFe10\text{-}1}$ film specimens.

the main compositions of the MFe particles are Na, Cl, and Fe elements. Meanwhile, much more volume contents of Vc powders were found on the E_{vc} series samples than those of the E_{Fe} and E_{MFe} series samples with the same weight loadings of Fe and MFe oxygen scavenger. Apparently, this is due to the density difference between the iron and ascorbic acid powders (7.8 g/cm^3 vs. 1.65 g/cm^3).

The SEM micrographs and EDX analysis of the compositions on the surfaces of typical E_{VcMFe} series

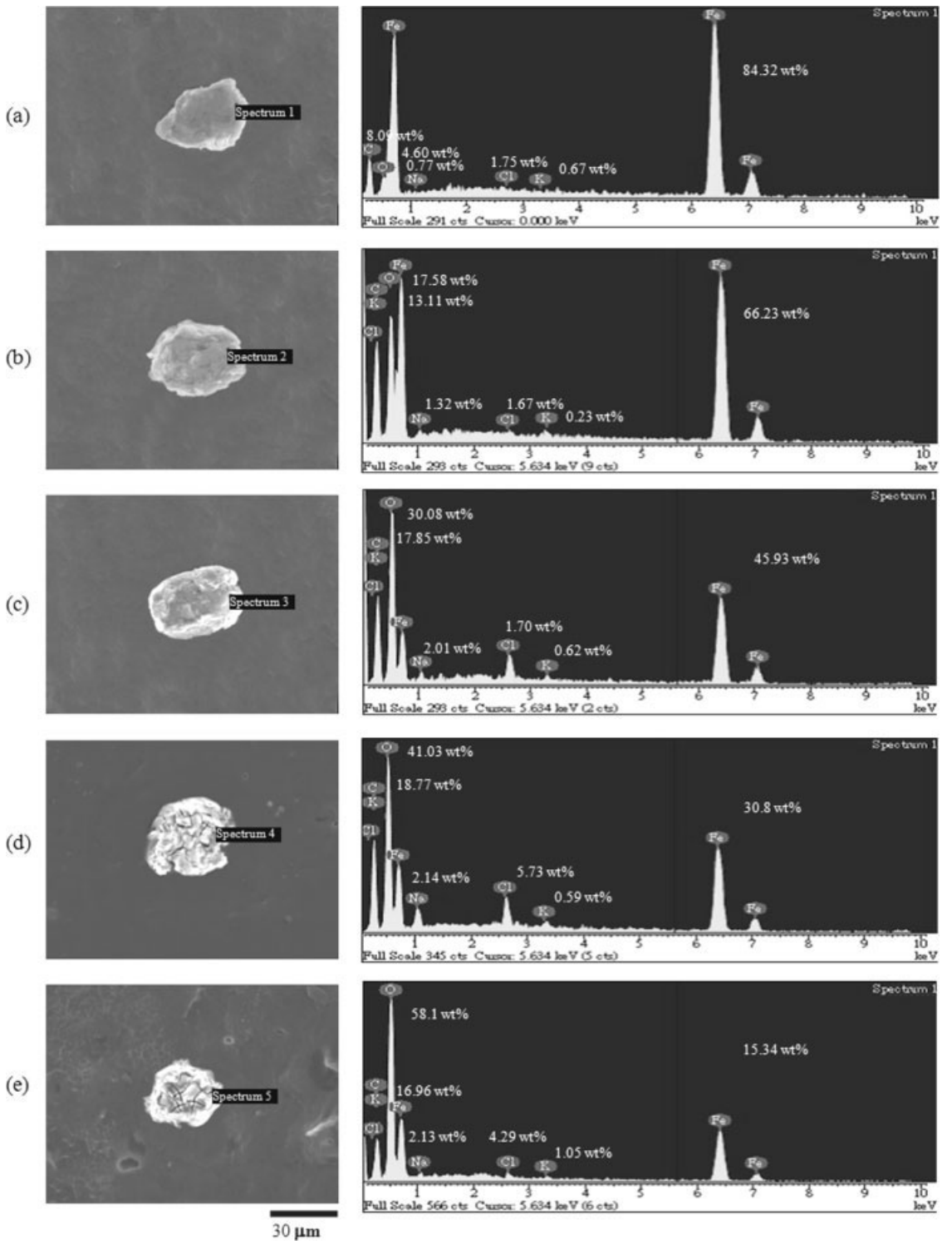

Figure 2 SEM micrographs of the fracture surfaces and EDX composition analysis of the particles present in (a) $E_{Vc1MFe9\text{-}30}$, (b) $E_{Vc3MFe7\text{-}30}$, (c) $E_{Vc5MFe5\text{-}30}$, (d) $E_{Vc7MFe3\text{-}30}$, (e) $E_{Vc9MFe1\text{-}30}$ film specimens.

samples are summarized in Figures 2–4. Similar to those found in E_{vc}, E_{Fe}, E_{MFe}, and E_{VcMFe} series samples, the MFe and Vc powders were relatively well distributed in $E_{Vc1MFe9\text{-}30}$ and $E_{Vc1MFe9\text{-}5}$ samples [see Figs. 2(a), 3(a), and 4(a)]. However, it is interesting to note that certain ascorbic acid powders were found surrounding but not over-wrapping on the surfaces of the MFe powders as the weight ratios of Vc to MFe present in the $E_{VcMFe\text{-}30}$ specimens are between 3/7 and 5/5. In fact, as shown in Figure 2(d,e), the MFe powders found in $E_{VcMFe\text{-}30}$ samples were nearly wrapped by the ascorbic acid powders

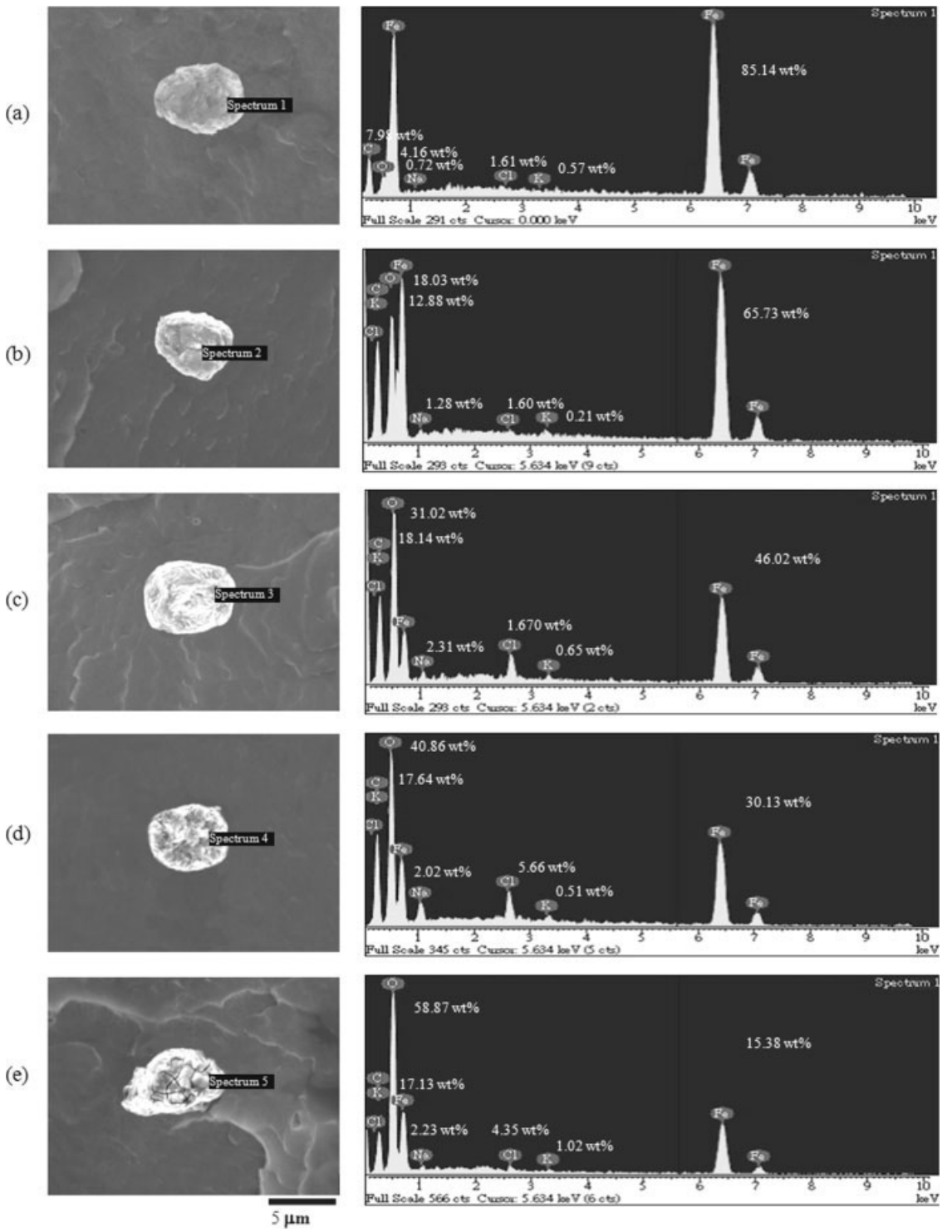

Figure 3 SEM micrographs of the fracture surfaces and EDX composition analysis of the particles present in (a) $E_{Vc1MFe9\text{-}5}$, (b) $E_{Vc3MFe7\text{-}5}$, (c) $E_{Vc5MFe5\text{-}5}$, (d) $E_{Vc7MFe3\text{-}5}$, (e) $E_{Vc9MFe1\text{-}5}$ film specimens.

as weight ratios of Vc to MFe are far more than 5/5 (i.e., $E_{Vc7MFe3\text{-}30}$ and $E_{Vc9MFe1\text{-}30}$ samples). Similar morphological characteristics were found in the $E_{VcMFe\text{-}5}$ and $E_{VcMFe\text{-}1}$ series samples, wherein the ascorbic acid powders were found not over-wrapping on the surfaces of the MFe powders in all $E_{VcMFe\text{-}1}$ and$E_{VcMFe\text{-}5}$series specimens with weight ratios of Vc to MFe between 3/7 and 7/3. Only at weight ratios of Vc to MFe more than 7/3, the MFe powders found in $E_{VcMFe\text{-}5}$ series specimens [see Fig. 3(e)] were nearly wrapped by the ascorbic acid powders, respectively.

At a fixed weight loading of Fe or MFe, the total surface areas of Fe or MFe are expected to increase

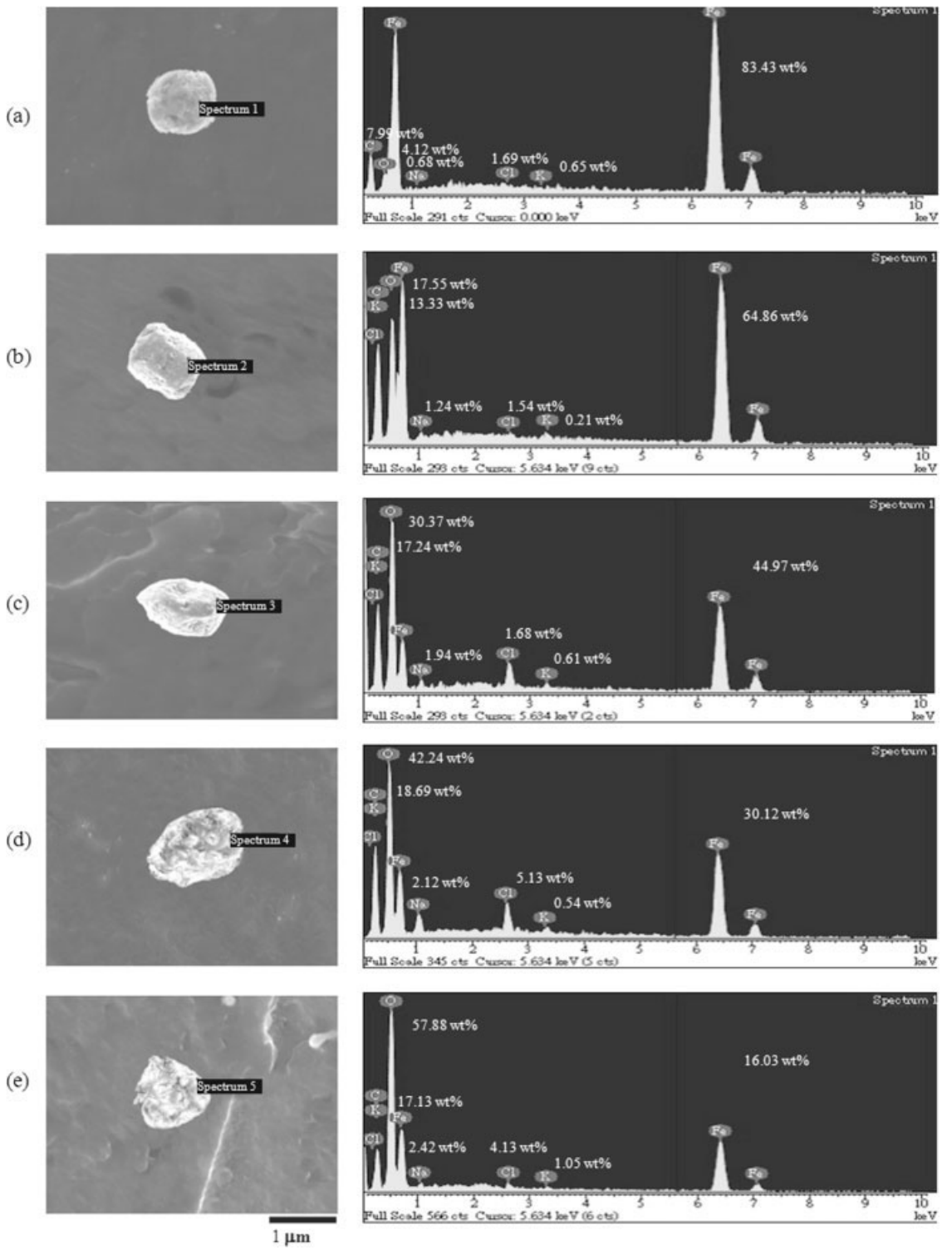

Figure 4 SEM micrographs of the fracture surfaces and EDX composition analysis of the particles present in (a) $E_{Vc1MFe9\text{-}1}$, (b) $E_{Vc3MFe7\text{-}1}$, (c) $E_{Vc5MFe5\text{-}1}$, (d) $E_{Vc7MFe3\text{-}1}$, (e) $E_{Vc9MFe1\text{-}1}$ film specimens.

as their particle sizes reduce. The theoretical surface areas of Fe (or MFe) powders with particle sizes of 5 or 1 μm are 5 or 29 times more than that of 30 μm Fe (or MFe) powders with the same weight loading, respectively. Presumably, smaller Fe (or MFe) powders with relatively higher surface areas require more ascorbic acids powders for full covering. Based on these premises, it is reasonable to understand that the critical Vc to MFe weight ratios for full covering of ascorbic acid powders on MFe powders increase from 5/5 to 7/3 as the original MFe particle sizes present in $E_{VcMFe\text{-}30}$ and$E_{VcMFe\text{-}5}$ series samples

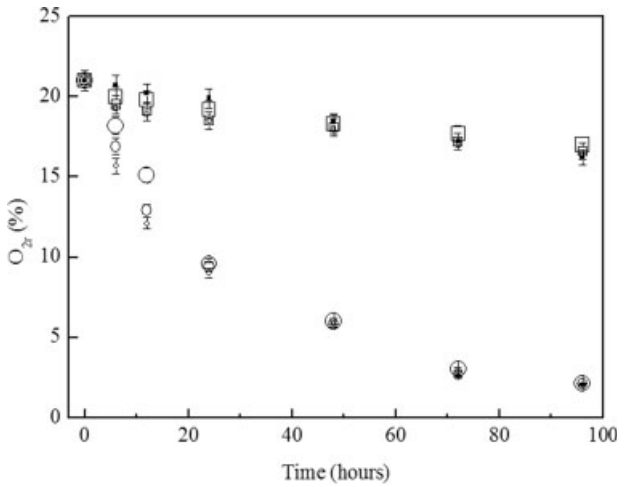

Figure 5 Residual oxygen concentrations (O_{2r}) present in the airtight conical flasks of E_{Vc10} (■), E_{Fe10-1} (□), E_{Fe10-5} (□), $E_{Fe10-30}$ (□), $E_{Fe10-50}$ (□), $E_{MFe10-1}$ (○), $E_{MFe10-5}$ (○), $E_{MFe10-30}$ (○), and $E_{MFe10-50}$ (○) film specimens.

reduce from 30 to 5 μm, respectively. In fact, nearly no over-wrapping MFe powders were found in all $E_{VcMFe-1}$ series specimens even with high values of Vc to MFe weight ratios (e.g., $E_{Vc9MFe1-1}$ specimen).

Oxygen depletion properties

The oxygen depletion properties of E_{Vc}, E_{Fe}, and E_{MFe} series samples placed in the airtight conical flasks are summarized in Figure 5. At a fixed loading of the Vc, Fe, and/or MFe oxygen scavengers, the residual oxygen concentrations (O_{2r}) present in the airtight flasks of each of the E_{Vc}, E_{Fe}, and E_{MFe} series samples reduce significantly as the testing time increases (see Fig. 5). Moreover, the oxygen depletion proceeds at a faster rate when the oxygen scavenger contents present in the E_{Vc} or E_{Fe} and E_{MFe} series samples increase, respectively. Similar to those found in our previous study,[48] the oxygen depletion rates of E_{Vc} and E_{Fe} series samples are significantly slower than those of E_{MFe} series samples with the same contents of oxygen scavengers. These interesting results are attributed to the fact that NaCl is well-known as an efficient catalyst for the oxidation of Fe powders can easily absorb water vapor[51] and substantially disassociates into Na^+ and Cl^- ions in the moisture-rich environment. Presumably, the substantially increased Na^+ and Cl^- ions can enhance the conductivity of the NaCl and Fe contained electrolytes and trigger Fe oxygen scavenger to an active state for further oxidation reaction. It is, therefore, reasonable to believe that the oxygen depletion rates of E_{MFe} series samples filled with MFe oxygen scavengers are much faster than those of E_{Fe} filled with pure Fe powders and E_{vc} series samples filled with ascorbic acid oxygen scavengers. In addition, it is interesting to note that the oxygen depletion rates of E_{Fe} and E_{MFe} series samples increase significantly as the particle sizes of MFe powders reduce (see Fig. 5). For instance, the O_{2r} values present in the airtight flask of $E_{MFe10-30}$, $E_{MFe10-5}$, and$E_{MFe10-1}$ specimens reduce to 18.2%/16.9%/15.7% and 15.1%/12.9% /12.1% after 6 and 12 h of oxygen depletion experiments, respectively. Even after more than 24 h of oxygen depletion experiments, the oxygen depletion rates of E_{MFe} series samples still increase diminutively as the MFe particle sizes reduce. Presumably, at a fixed loading of Fe or MFe, the total surface areas of Fe or MFe powders increase as their particle sizes reduce, respectively. The significantly improved surface areas of Fe or MFe oxygen scavengers are expected to react with oxygen and generate Fe^{2+} in a more efficient and fast way. It is, therefore, reasonable to believe that the oxygen depletion rates of E_{Fe} and E_{MFe} series samples increase significantly as the particle sizes of MFe powders reduce.

Figures 6–8 summarized the oxygen depletion properties of the E_{VcMFe} series samples, in which Vc together with varying sizes of MFe oxygen scavenger compounds were melt-blended in the EVA resins. As expected, the O_{2r} values present in the airtight flask of $E_{Vc1MFe9-30}$ sample at varying time are very close to the theoretical O_{2r} values estimated using "simple mixing rule." In contrast, the O_{2r} values present in the airtight flask of $E_{Vc3MFe7-30}$ and $E_{Vc5MFe5-30}$ samples are significantly lower than their theoretical O_{2r} values estimated using "simple mixing rule." However, at weight ratios of Vc to MFe higher than 5/5, the O_{2r} values present in the airtight flask of $E_{Vc7MFe3-30}$ and $E_{Vc9MFe1-30}$ specimens at varying time are significantly higher than their theoretical O_{2r} values estimated using "simple mixing rule" (see Fig. 6). Similar "synergistic" oxygen depletion properties was found in $E_{VcMFe-5}$ series samples, as their Vc/MFe weight ratios are between 3/7 and 7/3, wherein O_{2r} values present in the airtight flask of $E_{VcMFe-5}$ samples are significantly lower than their theoretical O_{2r} values estimated using "simple mixing rule" (see Fig. 7). Surprisingly, it is worth noting that the O_{2r} values present in the airtight flask of all $E_{VcMFe-1}$ series samples are significantly lower than their theoretical O_{2r} values estimated using "simple mixing rule" (see Fig. 8).

Furthermore, at a fixed weight ratio of Vc to MFe of the oxygen scavenger compounds, the oxygen depletion rates of E_{VcMFe} series samples increase significantly as the particle sizes of MFe powders reduce. For instance, after 24 h of oxygen depletion experiments, the O_{2r} values present in the airtight flasks of $E_{Vc3MFe7-x}$ series samples reduce from 10.1% to 8.0% to 7.2%, as their MFe particle sizes reduce from 30 to 5 μm to 1 μm (see Figs. 6–8), respectively. In fact, the $E_{Vc3MFe7-30}$, $E_{Vc3MFe7-5}$, and $E_{Vc3MFe7-1}$

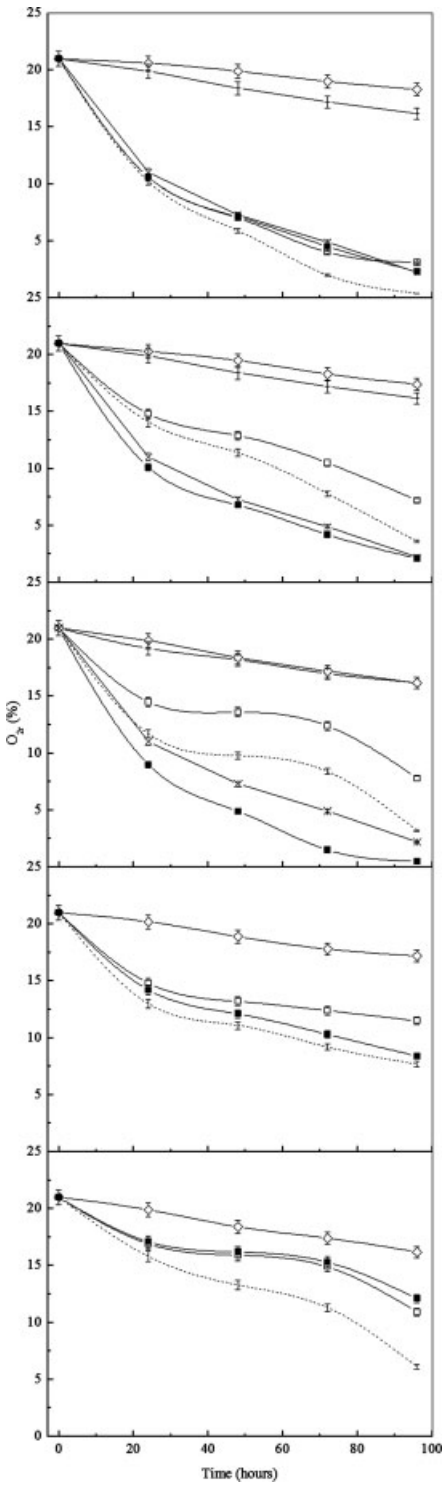

Figure 6 Residual oxygen concentrations (O_{2r}) present in the airtight conical flasks of (a) E_{Vc1} (◇), $E_{MFe9\text{-}30}$ (□), $E_{Vc1MFe9\text{-}30}$ (■), (b) E_{Vc3} (◇), $E_{MFe7\text{-}30}$ (□), $E_{Vc3MFe7\text{-}30}$ (■), E_{Vc10} (+), $E_{MFe10\text{-}30}$ (×), (c) E_{Vc5} (◇), $E_{MFe5\text{-}30}$ (□), $E_{Vc5MFe5\text{-}30}$ (■), E_{Vc10} (+), $E_{MFe10\text{-}30}$ (×), (d) E_{Vc7} (◇), $E_{MFe3\text{-}30}$ (□), $E_{Vc7MFe3\text{-}30}$ (■), and (e) E_{Vc9} (◇), $E_{MFe1\text{-}30}$ (□), $E_{Vc9M}E_{Fe1\text{-}30}$ (■) film specimens, respectively (The dashed line represents the theoretical oxygen concentrations present in the airtight flasks with $E_{VcMFe\text{-}30}$ series film specimens calculated using simple mixing rule.).

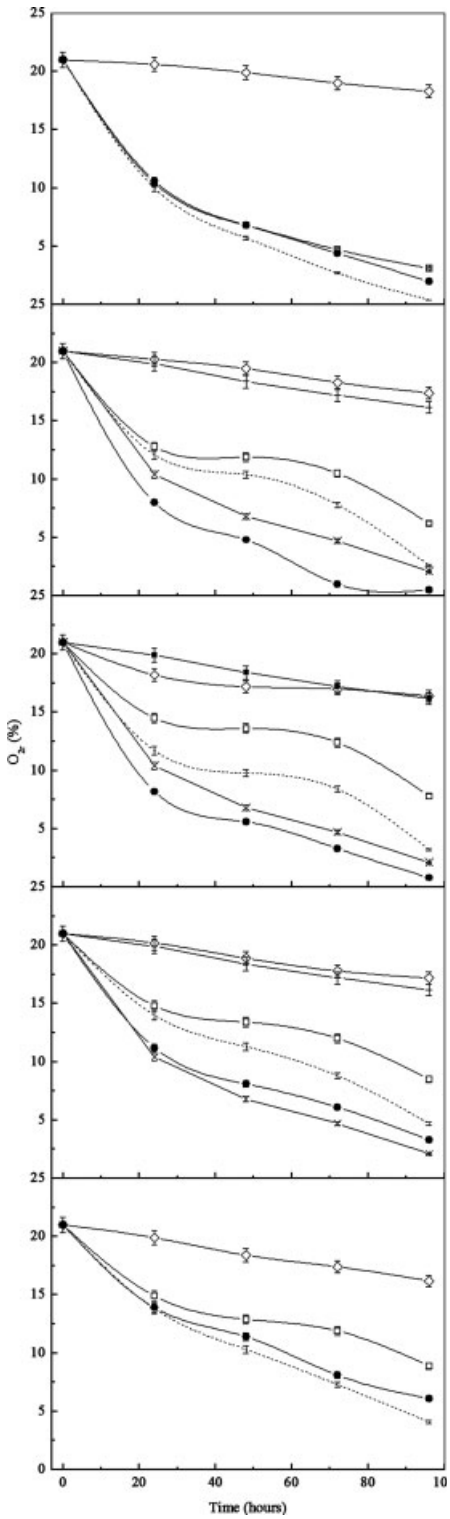

Figure 7 Residual oxygen concentrations (O_{2r}) present in the airtight conical flasks of (a) E_{Vc1} (◇), $E_{MFe9\text{-}5}$ (□), $E_{Vc1MFe9\text{-}5}$ (●), (b) E_{Vc3} (◇), $E_{MFe7\text{-}5}$ (□), $E_{Vc3MFe7\text{-}5}$ (●), E_{Vc10} (+), $E_{MFe10\text{-}5}$ (×), (c) E_{Vc5} (◇), $E_{MFe5\text{-}5}$ (□), $E_{Vc5MFe5\text{-}5}$ (●), E_{Vc10} (+), $E_{MFe10\text{-}5}$ (×), (d) E_{Vc7} (◇), $E_{MFe3\text{-}5}$ (□), $E_{Vc7MFe3\text{-}5}$ (●), E_{Vc10} (+), $E_{MFe10\text{-}5}$ (×), and (e) E_{Vc9} (◇), $E_{MFe1\text{-}5}$ (□), $E_{Vc9M}E_{Fe1\text{-}5}$ (●) film specimens, respectively (The dashed line represents the theoretical oxygen concentrations present in the airtight flasks with $E_{VcMFe\text{-}5}$ series film specimens calculated using simple mixing rule.).

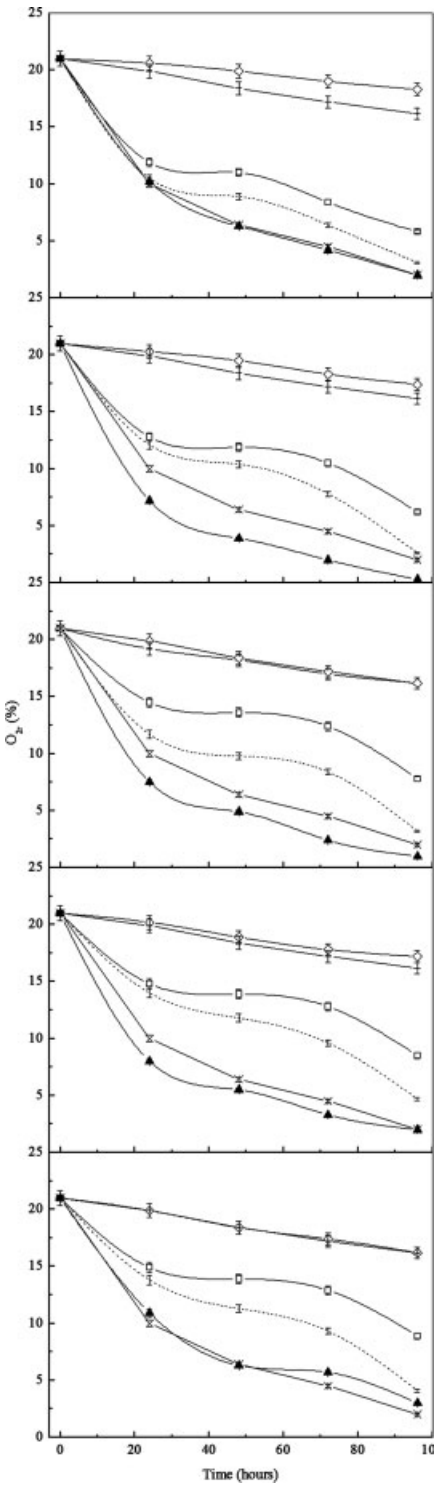

Figure 8 Residual oxygen concentrations (O_{2r}) present in the airtight conical flasks of (a) E_{Vc1} (◇), $E_{MFe9\text{-}1}$ (□), $E_{Vc1MFe9\text{-}1}$ (▲), E_{Vc10} (+), $E_{MFe10\text{-}1}$ (×), (b) E_{Vc3} (◇), $E_{MFe7\text{-}1}$ (□), $E_{Vc3MFe7\text{-}1}$ (▲), E_{Vc10} (+), $E_{MFe10\text{-}1}$ (×), (c) E_{Vc5} (◇), $E_{MFe5\text{-}1}$ (□), $E_{Vc5MFe5\text{-}1}$ (▲), E_{Vc10} (+), $E_{MFe10\text{-}1}$ (×), (d) E_{Vc7} (◇), $E_{MFe3\text{-}1}$ (□), $E_{Vc7MFe3\text{-}1}$ (▲), E_{Vc10} (+), $E_{MFe10\text{-}1}$ (×), and (e) E_{Vc9} (◇), $E_{MFe1\text{-}1}$ (□), $E_{Vc9M}E_{Fe1\text{-}1}$ (▲), E_{Vc10} (+), $E_{MFe10\text{-}1}$ (×) film specimens, respectively (The dashed line represents the theoretical oxygen concentrations present in the airtight flasks with $E_{VcMFe\text{-}1}$ series film specimens calculated using simple mixing rule.).

samples with a fixed weight ratio of Vc to MFe at 3/7 exhibit the "synergistic" and fastest oxygen depletion rates in each of the E_{VcMFe} series samples, respectively, wherein the O_{2r} values present in the airtight flask of $E_{Vc3MFe7\text{-}x}$ specimens at varying time are even lower than those of corresponding $E_{MFe10\text{-}x}$ specimens at varying time.

As reported by Miller and Buettner,[52] the Fe^{2+} ions generated during the oxidation process of Fe powders can serve as an effective catalyst for ascorbic acid to remove oxygen, wherein the ascorbic acid is oxidized by oxygen and transformed into water and dehydroascorbic acid. The water released after the oxidation of ascorbic acid can further enhance the oxidation of the Fe powders.[53] As shown in the previous section, the ascorbic acid powders were found surrounding but not over-wrapping on the surfaces of the MFe powders as the weight ratios of Vc to MFe present in the $E_{VcMFe\text{-}30}$ specimens are between 3/7 and 5/5. Similar surface morphology was found in the $E_{Vc3MFe7\text{-}5}$, $E_{Vc5MFe5\text{-}5}$, $E_{Vc7MFe3\text{-}5}$, and all $E_{VcMFe\text{-}1}$ series specimens. Presumably, the "synergistic" oxygen depletion properties of the oxygen-scavenging plastic film samples observed earlier are attributed to the "catalytic effect" caused by the optimum amounts of Fe^{2+} ions and water molecules formed during the oxidation processes of Fe and ascorbic acid powders. On the other hand, as mentioned in the previous section, at weight ratios of Vc to MFe more than 5/5 or 7/3, the MFe powders found in $E_{VcMFe\text{-}30}$ and $E_{VcMFe\text{-}5}$ series specimens (i.e., $E_{Vc7MFe3\text{-}30}$, $E_{Vc9MFe1\text{-}30}$, and $E_{Vc9MFe1\text{-}5}$) were nearly wrapped by the ascorbic acid powders, respectively. In contrast, $E_{VcMFe\text{-}1}$ series specimens were not overwrapped at all Vc/MFe weight ratios used in this study. The oxygen depletion properties of the overwrapped MFe powders can be significantly inhibited, since the MFe powders are barely exposed to the oxygen and water molecules and can not play as an effective oxygen scavenger. Under such circumstances, the amounts of Fe^{2+} ions generated may not be enough to serve as an effective catalyst for the oxidation of ascorbic acid powders. It is, therefore, reasonable to believe that the O_{2r} values of the $E_{Vc7MFe3\text{-}30}$, $E_{Vc9MFe1\text{-}30}$, and $E_{Vc9MFe1\text{-}5}$ specimens at varying time are significantly higher than their theoretical values estimated using "simple mixing rule."

Mechanical properties

The tensile properties of E_{Vc} and E_{MFe} series samples are summarized in Figures 9 and 10. The values of tensile strengths (σ_f) and elongations at break (ε_f) of E_{Vc} and E_{MFe} series samples decrease significantly as their Vc and MFe contents increase, respectively. It is worth nothing that, E_{MFe} series samples exhibit significantly higher σ_f and ε_f values than E_{Vc} series

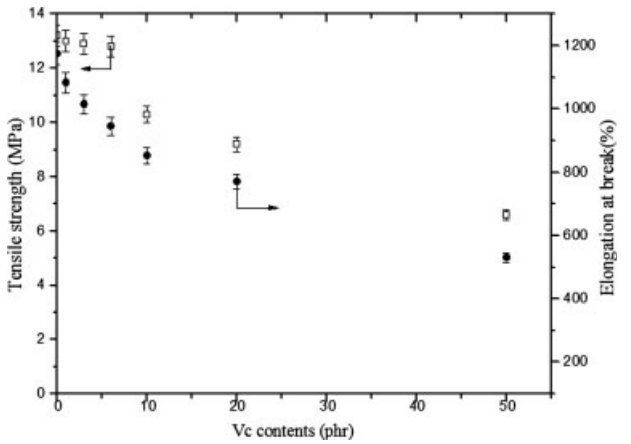

Figure 9 The tensile strengths (□) and elongations at break (●) of EVA and E_{Vc} specimens with varying contents of Vc powders.

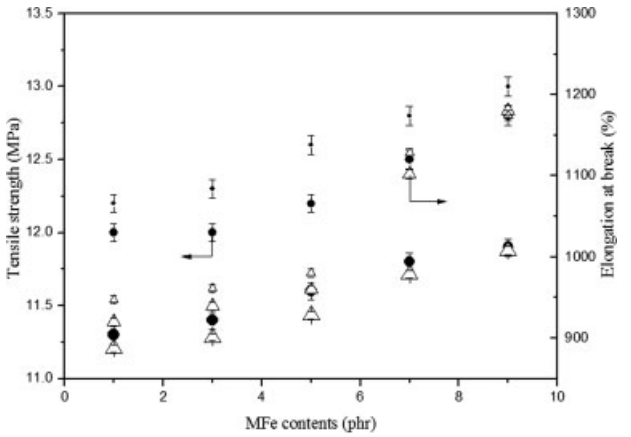

Figure 11 The tensile strengths and elongations at break of $E_{VcMFe-30}$ (●, △), $E_{VcMFe-5}$ (●, △), $E_{VcMFe-1}$ (●, △) specimens with 10 phr of oxygen scavenger compound of Vc and MFe powders.

samples with the same oxygen scavenger contents. As shown in Figure 10, the σ_f and ε_f values of the E_{MFe-30} series samples with 3–10 phr loadings of MFe powders are about 2.3–13.6% and 11.3–24.7% higher than those of the E_{Vc} series samples with the same weight loadings of Vc oxygen scavenger powders, respectively. Moreover, it is worth noting that, the σ_f and ε_f values of the E_{MFe} series samples with a fixed weight loading of MFe powders increase slightly as their MFe particle sizes present reduce (see Fig. 10). For instance, the σ_f and ε_f values of $E_{MFe10-x}$ series samples increase from 11.7MPa/1063.7% to 12.5 MPa/1083.7% and 12.8 MPa/1094.7%, as their MFe particle sizes reduce from 30 to 5 μm and 1 μm, respectively.

Figure 11 summarized the tensile properties of the E_{VcMFe} series samples with 10 phr of oxygen scavenger compounds of Vc and varying sizes of MFe powders. As shown in Figure 11, the σ_f and ε_f values of each E_{VcMFe} series samples increase significantly as the Vc loadings present in the oxygen scavenger compounds decrease. For instance, the σ_f and ε_f values of $E_{VcMFe-30}$ series samples increase from 11.3 MPa/887.3% to 11.9 MPa/1007.7%, as the weight ratios of Vc to MFe decrease from 9/1 to 1/9. On the other hand, at a fixed weight ratio of Vc to MFe, the σ_f and ε_f values of each E_{VcMFe} series samples with 10 phr Vc/MFe oxygen scavenger compounds increase significantly as their MFe particle sizes reduce. For instance, the σ_f and ε_f values of $E_{Vc5MFe5-x}$ series samples increase from 11.6 MPa/928.1% to 12.2 MPa/960.0% and 12.6 MPa/980.1%, as their MFe particle sizes reduce from 30 to 5 μm and 1 μm, respectively.

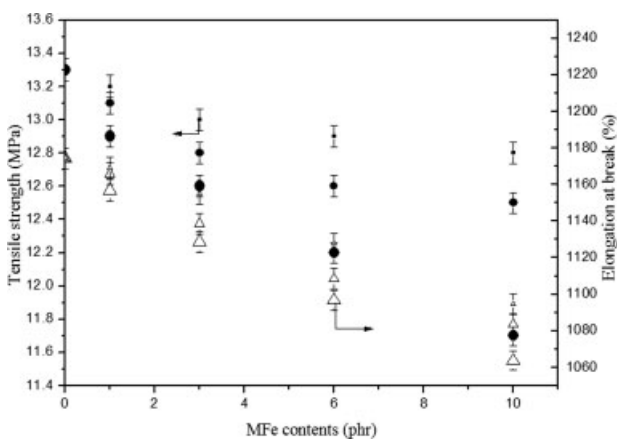

Figure 10 The tensile strengths and elongations at break of E_{MFe-30} (●, △), E_{MFe-5} (●, △), and E_{MFe-1} (●, △) specimens with varying contents of MFe powders.

Presumably, during the tensile experiments of the oxygen scavenger compounds filled EVA specimens, the presence of oxygen scavenger powers can cause "stress concentration" and "early breakage of EVA molecules" at the boundaries between oxygen scavenger powders and the EVA resins, since the interfacial adhesion between the scavenger powders and EVA resins is poor. The degree of stress concentration is expected to increase as the loadings and sizes of the fillers increase. It is, therefore, reasonable to expect that the σ_f and ε_f values of the E_{Vc} and E_{MFe} series samples continue to reduce with increasing the oxygen scavenger contents and particle sizes. However, as mentioned previously, the density of the iron powders is much higher than that of the ascorbic acid powders (7.8 g/cm^3 vs. 1.65 g/cm^3). The volumes of the Fe and MFe powders are much smaller than those of the ascorbic acid powders with the same weights. By the same analogy, the volumes of 10-phr oxygen scavenger compounds present in the E_{VcMFe} series samples can reduce significantly as the MFe contents present in the oxygen scavenger compounds increase. The degree of "stress concentration" and "early breakage of EVA molecules" at

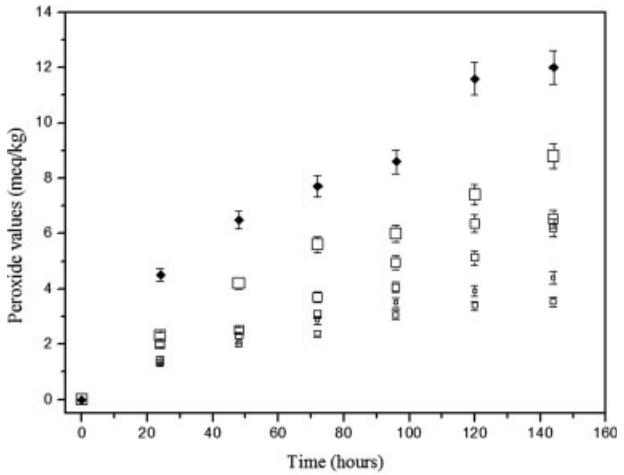

Figure 12 The peroxide values of the model food placed in airtight conical flasks of EVA (◆), $E_{Vc1MFe9\text{-}30}$ (□), $E_{Vc3MFe7\text{-}30}$ (□), $E_{Vc5MFe5\text{-}30}$ (□), $E_{Vc7MFe3\text{-}30}$ (□), and $E_{Vc9MFe1\text{-}30}$ (□) film specimens.

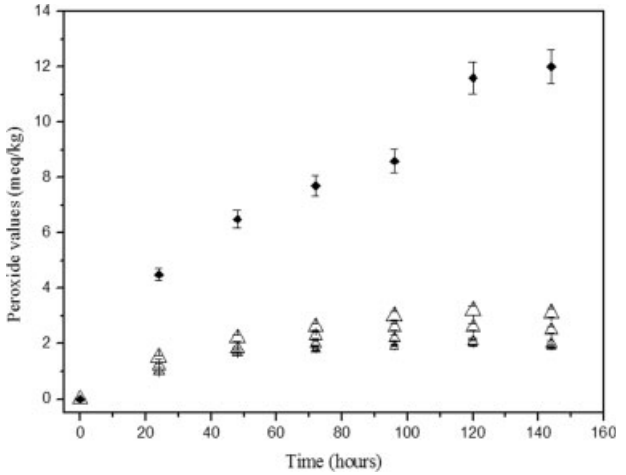

Figure 14 The peroxide values of the model food placed in airtight conical flasks of EVA (◆), $E_{Vc1MFe9\text{-}1}$ (△), $E_{Vc3MFe7\text{-}1}$ (△), $E_{Vc5MFe5\text{-}1}$ (△), $E_{Vc7MFe3\text{-}1}$ (△), and $E_{Vc9MFe1\text{-}1}$ (△) film specimens.

the boundaries is expected to reduce as the volumes of the oxygen scavengers reduce. As a consequence, E_{Fe} and E_{MFe} series samples always exhibit higher σ_f and ε_f values than the E_{Vc} series samples with the same oxygen scavenger contents. Similarly, it is reasonable to understand that the σ_f and ε_f values of the E_{VcMFe} series samples increase significantly as the contents of MFe present in the 10-phr oxygen scavenger compounds increase.

Analysis of the lipid oxidation of the modeled food sample

Figures 12–14 summarized the peroxide values (POVs) of modeled food samples placed in airtight conical flasks with EVA and $E_{VcMFe\text{-}x}$ series film specimens at 30°C for varying amounts of time. As

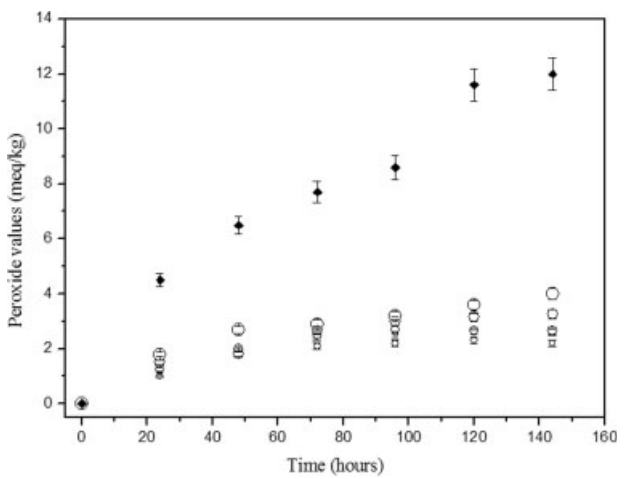

Figure 13 The peroxide values of the model food placed in airtight conical flasks of EVA (◆), $E_{Vc1MFe9\text{-}5}$ (○), $E_{Vc3MFe7\text{-}5}$ (○), $E_{Vc5MFe5\text{-}5}$ (○), $E_{Vc7MFe3\text{-}5}$ (○), and $E_{Vc9MFe1\text{-}5}$ (○) film specimens.

expected, the peroxide values of modeled food samples increase as the testing time increases, which are attributed to the oxidative deterioration of lipids with increasing testing time. In contrast, the peroxide values of modeled food samples tested in airtight flasks of $E_{VcMFe\text{-}x}$ series film specimens are always significantly lower than that of EVA film specimen tested for the same storage time. Moreover, the lowest peroxide value of modeled food samples present in each conical flask of $E_{VcMFe\text{-}x}$ series samples was always found at the 3/7 "optimum" weight ratio of Vc to MFe, respectively, wherein the lowest peroxide value found in each conical flask of $E_{VcMFe\text{-}x}$ series samples reduce significantly with decreasing in their original MFe particle sizes. For instance, the peroxide values of modeled food samples present in airtight flasks of $E_{Vc3MFe7\text{-}x}$ specimens reduce from 2 to 1.8 meq/kg and 1.7 and from 3.5 to 2.2 meq/kg and 1.9 meq/kg after 48 and 144 h of lipid oxidation experiments, as their original MFe particle sizes reduce from about 30 to 5 μm to 1 μm, respectively. In fact, in consistent with the oxygen depletion properties found in the previous section, the POVs of modeled food samples present in the airtight flask with $E_{VcMFe\text{-}x}$ series samples reduce significantly as their oxygen depletion properties improve. Based on the lipid oxidation analysis of the modeled food samples, it is reasonable to believe that the oxygen absorbable E_{VcMFe} samples can act as efficient oxygen-scavenging resins to prevent modeled food samples from lipid oxidation.

CONCLUSIONS

The oxygen depletion experiments exhibit that the oxygen depletion rates of modified iron powders filled E_{MFe} series samples are much faster than those

of E_{Vc} or E_{Fe} series samples filled with the same weight loadings of ascorbic acid or pure iron powders, wherein the oxygen depletion rates of E_{Fe} or E_{MFe} series samples increase significantly as their original particle sizes of Fe or MFe powders reduce. After blending Vc together with varying sizes of MFe in the EVA resins, "synergistic" oxygen depletion properties were found in each $E_{VcMFe-30}$, $E_{VcMFe-5}$, and $E_{VcMFe-1}$ series samples, as their weight ratios of Vc to MFe are between 3/7 to 5/5, 3/7 to 7/3 and 1/9 to 9/1, respectively. Similarly, at a fixed weight ratio of Vc to MFe, the oxygen depletion rates of E_{VcMFe} series samples increase significantly as their particle sizes of MFe powders reduce. For instance, after 96 h of oxygen depletion experiments, the O_{2r} values present in the airtight flasks of $E_{Vc3MFe7-30}$, $E_{Vc3MFe7-5}$ and $E_{Vc3MFe7-1}$ samples are 55.5, 61.7, and 62.3% higher than that of the E_{Vc3} sample, respectively. The lipid oxidation experiments of modeled food samples suggest that E_{VcMFe} series samples are efficient oxygen-scavenging resins that can prevent modeled food samples from lipid oxidation. In fact, the oxygen-scavenging resins with better oxygen depletion properties always result in lower POVs for modeled food samples stored in the airtight flasks of E_{VcMFe} series samples.

Further SEM and EDX analysis of the compositions on the surfaces of each $E_{VcMFe-x}$ series samples indicate that the ascorbic acid powders were found surrounding but not over-wrapping on the surfaces of the MFe powders as their Vc/MFe weight ratios are between certain specific ranges, wherein "synergistic" oxygen depletion properties were always found in each $E_{VcMFe-x}$ series samples. In contrast, at Vc/MFe weight ratios higher than the values of these specific ranges, the MFe powders found in the $E_{Vc7MFe3-30}$, $E_{Vc9MFe1-30}$, and $E_{Vc9MFe1-5}$ specimens were nearly wrapped by the ascorbic acid powders. Presumably, the oxygen depletion properties of MFe powders can be significantly inhibited after they were over-wrapped, since oxygen and water molecules can no longer enter into the over-wrapped MFe powders easily, which can not only reduce the inherent oxygen depletion properties of MFe powders but also can inhibit the oxygen depletion properties of Vc powders without releasing the catalytic Fe^{2+} from MFe powders.

As expected, σ_f and ε_f values of E_{Vc} and E_{MFe} series samples reduce significantly as their MFe and Vc contents increase, respectively. In contrast, σ_f and ε_f values of E_{VcMFe} series samples increase significantly as their Vc loadings decrease. Apparently, this is due to the fact that the volumes of the MFe powders are much smaller than those of the ascorbic acid powders with the same weight loadings. On the other hand, at a fixed weight ratio of Vc to MFe, the σ_f and ε_f values of each E_{VcMFe} series samples with 10 phr Vc/MFe oxygen scavenger compounds increase significantly as their MFe particle sizes reduce. Presumably, during the tensile experiments, the degree of stress concentration and "early breakage" of EVA molecules at the boundaries between oxygen scavenger powders and the EVA resins is expected to reduce as the volume loadings and sizes of the fillers reduce.

References

1. Lin, S.; Hsieh, F.; Huff, H. E. Anim Feed Sci Technol 1998, 71, 283.
2. Brooks, S. P. J.; Lampi, B. J. J Nutr Biochem 2001, 12, 422.
3. Malecka, M. Food Chem 2002, 79, 327.
4. Rehman, Z.-U.; Habib, F.; Shah, W. H. Food Chem 2004, 85, 215.
5. Ekstrand, B.; Gangby, I.; Åkesson, G.; Stollman, U.; Lingnert, H.; Dahl, S. J Cereal Sci 1993, 17, 247.
6. Skibsted, L. H.; Mikkelsen, A.; Bertelsen, G. In Flavour of Meat, Meat Products and Sea Foods; Shahidi, F., Ed.; Blackie Academic & Professional: London, 1998; p 217.
7. Morrissey, P. A.; Sheehy, P. J. A.; Galvin, K.; Kerry, J. P.; Buckley, D. J. Meat Sci 1998, 49, 76.
8. Suzuki, Y.; Ise, K.; Li, C.; Honda, I.; Iwai, Y.; Matsukura, U. J Agric Food Chem 1999, 47, 1119.
9. Cumbee, B.; Hildebrand, D. F.; Addo, K. J Food Sci 1997, 62, 281.
10. Champagne, E.; Grimm, C. Cereal Chem 1995, 72, 255.
11. Wessling, C.; Nielsen, T.; Giacin, J. R. J Sci Food Agric 2001, 81, 194.
12. Vermeiren, L.; Devlieghere, F.; Van Beest, M.; de Kruijf, N.; Debevere, J. Trends Food Sci Technol 1999, 10, 77.
13. Yeh, J. T.; Huang, S. S.; Yao, W. H.; Macromol Mater Eng 2002, 287, 532.
14. Yeh, J. T.; Fan-Chiang, C. C.; Cho, M. F. Polym Bull 1995, 35, 371.
15. Yeh, J. T.; Fan-Chiang, C. C.; Yang, S. S. J Appl Polym Sci 1997, 64, 1531.
16. Yeh, J. T.; Fan-Chiang, C. C. J Appl Polym Sci 1997, 66, 2517.
17. Yeh, J. T.; Fan-Chiang, C. C. J Polym Res 1996, 3, 211.
18. Yeh, J. T.; Jyan, C. F. Polym Eng Sci 1998, 38, 1482.
19. Yeh, J. T.; Chao, C. C.; Chen, C. H. J Appl Polym Sci 2000, 76, 1997.
20. Yeh, J. T.; Chang, S. S.; Yao, H. T.; Chen, K. N.; Jou, W. S. J Mater Sci 2000, 35, 1321.
21. Yeh, J. T.; Yang, S. S.; Jyan, C. F.; Chou, S. Polym Eng Sci 1999, 39, 1952.
22. Yeh, J. T.; Huang, S. S.; Chen, H. Y. Polym Eng Sci 2005, 45, 25.
23. Yeh, J. T.; Yao, W. H.; Du, Q. G.; Chen, C. C. J Polym Sci Polym Phys Ed 2005, 43, 511.
24. Yeh, J. T.; Shih, W. H.; Huang, S. S. Macromol Mater Eng 2002, 287, 23.
25. Wessling, R. A. Polyvinylidene Chloride; Gorden and Breach Science Publishers: New York, 1977.
26. Inoue, Y.; Komatsu, T. U.S. Pat. 4,908,151 (1990).
27. Gabrielle, M. C. Mod Plast 1999, 76, 73.
28. Zimmerman, P. L.; Ernst, L. J.; Ossian, W. F. Food Technol 1974, 28, 103.
29. Berenzon, S.; Saguy, I. S. Food Sci Technol 1998, 31, 1.
30. Venkateshwaran; Lakshmi, N. U.S. Pat. 5,744,056 (1998).
31. Farrell, C. J.; Tsai, B. C., U.S. Pat. 4,536,409 (1985).
32. Ohtsuka, S.; Komatsu, T.; Kondoh, Y.; Takahashi, H. U.S. Pat. 448,513,3 (1984).
33. Edens, L. V.; Farin, F. R.; Ligtvoet, A. F. D.; Van, D. P.; Johannes, B. L. U.S. Pat. 5,106,633 (1992).

34. Zenner, B. D. U.S. Pat. 6,391,406 (2002).
35. Graf, E. U.S. Pat. 5,284,871 (1994).
36. Rooney, M. L. J Food Sci 1981, 47, 291.
37. Nakamura, H.; Hoshino, J. Techniques for the Preservation of Food by Employment of an Oxygen Absorber; Technical information Mitsubishi Gas Chem Co.: Tokyo, Ageless Division, 1983; p 1.
38. Klein, T.; Knorr, D. J Food Sci 1990, 55, 869.
39. Labuza, T. P. Food Res 1987, 32, 276.
40. Teumac, F. N.; Zenner, B. D. U S Pat. 6,465,065 (2002).
41. Graf, E. U S Pat. 5,270,337 (1993).
42. Graf, E. J Agric Food Chem 1994, 42, 1616.
43. Labuza, T. P. Food Sci Technol Today 1990, 4, 53.
44. Aaron, L. B.; Eugene, R. S.; Lauri, R. K. Active Packaging for Food Application; Technomic Pub. Co.: Lancaster, 2001.
45. Cook, P. In International Food Technologists Annu Meeting Book of Abstracts; IFT: Atlanta, GA, 1998; p 26.
46. Rooney, M. L. In International Food Technologists Annu Meeting Book of Abstracts, IFT: New Orleans, LA, 2001.
47. Tewari, G.; Jayas, D. S.; Jeremiah, L. E.; Holley, R. A. Int J Food Sci Technol 2002, 37, 209.
48. Yeh, J. T.; Cui, L.; Tsai, F. C.; Chen, K. N. J Polym Eng 2007, 27, 245.
49. Wunderlich, B. Macromolecular Physics; Academic: New York, 1973; Vol. 1, 388.
50. Teraoka, R.; Otsuka, M.; Matsuda, Y. Pharm Res 1994, 11, 1077.
51. Graedel, T. E.; Frankenthal, R. P. J Electrochem Soc 1990, 137, 2385.
52. Miller, D. M.; Buettner, G. R.; Aust, S. D. Free Radic Biol Med 1990, 8, 95.
53. Smith, J. P.; Ramaswamy, H. S.; Simpson, B. K. Trends Food Sci Technol 1990, 11, 111.